Fermi National Accelerator Laboratory

FERMILAB-Pub-78/26-EXP
7420.045

(Submitted to Phys. Rev. D)

INCLUSIVE NEUTRAL STRANGE PARTICLE PRODUCTION FROM HIGH ENERGY νp CHARGED-CURRENT INTERACTIONS

J. P. Berge, D. V. Bogert, D. C. Cundy, F. A. DiBianca, R. J. Endorf, R. Hanft, C. Kochowski, J. A. Malko, G. I. Moffatt, F. A. Nezrick, W. G. Scott, and W. Smart
Fermi National Accelerator Laboratory, Batavia, Illinois 60510

and

G. R. Lynch, J. P. Marriner, and M. L. Stevenson
University of California, Berkeley, California 94720

and

R. J. Cence, F. A. Harris, M. Jones, S. I. Parker, M. W. Peters, V. Z. Peterson, and V. J. Stenger
University of Hawaii, Honolulu, Hawaii 96822

and

J. Bell, C. T. Coffin, R. N. Diamond, H. T. French, W. C. Louis, B. P. Roe, R. T. Ross, A. A. Seidl, J. C. Vander Velde, and E. Wang
University of Michigan, Ann Arbor, Michigan 48109

March 1978

FERMILAB-Pub-78/26-EXP

INCLUSIVE NEUTRAL STRANGE PARTICLE PRODUCTION FROM HIGH ENERGY νp CHARGED-CURRENT INTERACTIONS*

J. P. Berge, V. D. Bogert, D. C. Cundy,[a] F. A. DiBianca,[b]
R. J. Endorf,[c] R. Hanft, C. Kochowski,[d] J. A. Malko,
G. I. Moffatt, F. A. Nezrick, W. G. Scott,[e] and W. Smart
Fermi National Accelerator Laboratory
Batavia, Illinois 60510 USA

G. R. Lynch, J. P. Marriner, and M. L. Stevenson
University of California
Berkeley, California 94720

R. J. Cence, F. A. Harris, M. Jones, S. I. Parker,
M. W. Peters, V. Z. Peterson, and V. J. Stenger
University of Hawaii
Honolulu, Hawaii 96822

J. Bell, C. T. Coffin, R. N. Diamond,[f] H. T. French,[g]
W. C. Louis, B. P. Roe, R. T. Ross, A. A. Seidl,
J. C. Vander Velde, and E. Wang
University of Michigan
Ann Arbor, Michigan 48109

*Work supported in part by the U.S. Department of Energy and the National Science Foundation.

[a]Permanent address: CERN, 1211 Geneva 23, Switzerland.

[b]Present address: General Electric Medical Systems Division, P. O. Box 414, Milwaukee, Wisconsin 53201.

[c]Permanent address: Centre d'Etudes Nucleaires de Saclay, B. P. No. 2, F-91190 Gif-sur-Yvette

[e]Present address: CERN, 1211 Geneva 23, Switzerland.

[f]Present address: Florida State University Tallahassee, Florida 32306

[g]Present address: Columbia University, New York, New York 10027.

ABSTRACT

We have studied the properties of inclusive neutral strange particle production in charged-current νp interactions. The rate for producing at least one neutral strange particle in a charged-current interaction is 0.14 ± 0.02 The inclusive distributions for events with neutral strange particles and for all charged-current events exhibit the same qualitative behavior. We find no acceptable candidates for the $\Delta S = -\Delta Q$ Λ production reaction $\nu p \rightarrow \mu^- \Lambda 3\pi^+\pi^-$ in approximately 3000 charged-current events with $E_\nu > 10$ GeV. We find upper limits (relative to the total charged-current sample) for charmed particle production in any one mass region with subsequent decay into Λmπ and Kmπ final states of 1% and 2% respectively.

I. INTRODUCTION

We have collected a sample of charged-current νp events having a visible neutral strange particle decay in the final state $\nu p \to \mu^- V^o X^{++}$, where V^o stands for $\Lambda \to p\pi^-$, $K_S^o \to \pi^+\pi^-$ or $\bar{\Lambda} \to \bar{p}\pi^+$, and X^{++} is the hadronic system of charged +2. The general features of the production mechanism of this data sample have been studied in terms of variables used in weak and strong interaction physics. We have also searched for evidence of charmed particle production in our data.

In Section II we discuss the experimental details of the event selection. Section III deals with inclusive neutral strange particle production rates. Inclusive single-particle distributions are presented in Section IV, and in Section V we discuss a search for charmed particle signals in invariant mass distributions. The major conclusions are summarized in Section VI.

II. EVENT SELECTION

The data come from two separate exposures of the Fermilab 15' hydrogen-filled bubble chamber to high energy neutrino beams. The first (second) exposure of 70,000 (80,000) pictures was made with a wide-band one-horn (two-horn) focused beam with

0.52×10^{18} (0.60×10^{18}) protons at 300 (400) GeV on target. Adding the two exposures results in a smoothly varying neutrino energy spectrum which peaks at ~15 GeV and decreases quickly thereafter (~90% of the flux is below 100 GeV).

The film was scanned for all neutral-induced interactions. After measuring and processing through geometrical reconstruction programs the events were reexamined on the scan table by physicists. Events found to originate from interactions in the chamber wall or from another upstream event were removed from the sample. To study the inclusive V^o production we then processed through kinematics those events having one or more possible associated two-prong decays. For all fits we have employed a confidence level cut of 0.001. We took a V^o to be a γ conversion if it had a constrained γ fit for which the e^+ momentum transverse to the V^o direction was less than 20 MeV. The few Λ/K ambiguities (~8% of the V^o decays) were taken as Λ's. In addition we ignored any fit corresponding to a decay with a proper time τ greater than five lifetimes. The distributions of $c\tau$ and $\cos\theta$ are shown in figures 1 and 2 for the 161 $\Lambda \to p\pi^-$ and 230 $K^o_s \to \pi^+\pi^-$ decays thus selected. For the $\Lambda(K^o_s)$ decay, θ is the angle between the decay proton (π^+) and the V^o direction calculated in the V^o rest frame. Except for a possible small loss at low $c\tau$ the distributions in Fig. 1 are in excellent agreement with the known lifetimes (solid curves), while the angular distributions in Fig. 2 are consistent with being isotropic.

The charged-current events were obtained by requiring that there be three or more prongs at the primary vertex, that the

sum of the visible momentum along the incoming neutrino direction (ΣP_x) be greater than 10 GeV/c and that there be a selected muon. The muons were selected by a Monte Carlo tested algorithm which basically identifies the μ^- candidate as being the negative track with the highest transverse momentum relative to the neutrino direction.[1] If the track thus selected is found to interact, the event is rejected as a charged-current event. The above selection results in a charged-current ν sample of ~2300 events with less than ~5% contamination from neutral current and $\bar{\nu}$ charged-current events. We estimate that ~17% of the charged-current events have been lost due to the muon selection algorithm. The incident K_L^o background is determined by using fits to the $K_L^o p \to K_S^o p\pi^+\pi^-$ channel and is found to be ~1/2% of the charged-current sample for $\Sigma P_x > 10$ GeV/c.

The energy of the incident neutrino, E_ν, is estimated by using a modification of a method due to Grant.[2] The results presented in this paper are not significantly sensitive to the particular energy estimation method employed. Requiring $E_\nu >$ 10 GeV gives us a charged-current V^o sample of 132 events. The reconstructed neutrino energy E_ν and charged multiplicity for these events are shown in Fig. 3. Table I gives a break-down of these 132 events in terms of their assignments to $1V^o$, $2V^o$ and $3V^o$ final states.[3] The two $3V^o$ events have at least three strange particles in the final state, or if we assume $\Delta S = 0$, they probably have four strange particles. Both events are of high energy ($E_\nu > 50$ GeV/c) and are therefore unlikely to be produced by incident strange hadrons.[4]

III. PRODUCTION RATES

In Table II we show the corrected number of strange particle events for various $1V^o$, $2V^o$ and $3V^o$ final states. In obtaining these numbers we have assumed that the data result from the following six channels: $\nu p \to \mu^- \Lambda X^{++}$; $\nu p \to \mu^- \Lambda K^o X^{++}$, $\nu p \to \mu^- \Lambda K^o K^o X^{++}$; $\nu p \to \mu^- \Lambda\Lambda K^o X^{++}$; $\nu p \to \mu^- K^o K^o X^{++}$; $\nu p \to \mu^- K^o X^{++}$. Here X^{++} does not contain a neutral strange particle. We then assume that K^o is 1/2 K_S^o and 1/2 K_L^o, and calculate how each of these channels feeds into the events with 1, 2 and 3 observed V^o decays. The numbers have been corrected for neutral decay modes and minimum and maximum potential length cuts of 0.5 cm and 20 cm respectively at the V^o decay vertex. The large relative errors in certain channels are due to the strong $1V^o$, $2V^o$, and $3V^o$ correlations. The one observed $\Lambda K_S^o K_S^o$ event, for example, predicts four observed ΛK_S^o events. The rate for events with one or more V^o's normalized to the total charged-current sample is

$$\frac{\nu p \to \mu^- V^o X^{++}}{\nu p \to \mu^- X^{++}} = 0.14 \pm 0.02$$

for $E_\nu > 10$ GeV. This rate may be compared to charged-current strange particle production rates found in other experiments with approximately the same beam energy spectrum: 0.21 ± 0.04 for $\bar{\nu}p$ interactions[5] and 0.16 ± 0.03 for $\bar{\nu}$ neon interactions.[6]

The ratio of the number of events containing at least one Λ to the number of events containing at least one K^o is 0.59 ± 0.10. For $\bar{\nu}p$ interactions this ratio is 0.40 ± 0.16.[5]

Since the identification efficiency for charged K's is low, it is in general not possible to obtain an estimate of the amount of associated and non-associated production present in our data. However, we may estimate the number of $\Delta S = -\Delta Q$ events which contain a Λ by assuming equal rates for $\nu p \to \mu^- \Lambda K^o X^{++}$ and $\nu p \to \mu^- \Lambda K^+ X^+$. In this way we obtain a Λ production from $\Delta S = -\Delta Q$ of 3.9 ± 1.5% of the total charged-current rate. The assumption of equal rates for $\nu p \to \mu^- \Lambda K^o X^{++}$ and $\nu p \to \mu^- \Lambda K^+ X^+$ is only a rough estimate and may in fact be a gross underestimate for K^+ production.[7] To make the $\Delta S = -\Delta Q$ rate fall within 1.5 σ of zero we need to make the ratio $(\mu^- \Lambda K^+ X^+)/(\mu^- \Lambda K^o X^{++})$ equal to 3. This is in fact not an unreasonable value for the ratio and illustrates that in this experiment inclusive Λ production does not allow us to obtain a reliable rate for $\Delta S = -\Delta Q$ production.

The $\Lambda\gamma$ invariant mass distribution presented in Fig. 4 indicates Σ^o production. The Σ^o signal accounts for between 50 and 100% of the Λ production, where we have used an average γ-conversion probably of 13%. In the following when we refer to Λ production we include this Σ^o production.

The $\Lambda\pi^\pm$ and $K^o_s \pi^\pm$ mass distributions are shown in figures 5(a)-5(d). There is a clear signal for $\Sigma^+(1385)$ in Fig. 5(a). This signal of approximately 12 events above background corresponds to ~1% of the total charged-current sample.

Figure 5(a) also gives some indication for broad enhancements at ~1.55 and 1.85 GeV. These enhancements are seen more clearly in Fig. 6 where the data is presented in 50 MeV bins. We note that our resolution is ~10 MeV and therefore the enhancements cannot be due to narrow $\Lambda\pi^+$ states. A possible interpretation[9] is that the effect at 1.85 GeV is due to the $\Sigma^0\pi^+$ decay of the $\Sigma^+(1920)$ and the effect at 1.55 GeV is due to the $\Sigma^0\pi^+$ decay of the $\Sigma(1670)$. With this interpretation and assuming a 35[25] % branching ratio[9] for $\Sigma^+(1920) \to \Sigma^0\pi^+[\Sigma^+(1670) \to \Sigma^0\pi^+]$ we obtain a production rate of ~3% of the charged-current sample for both the $\Sigma^+(1920)$ and the $\Sigma^+(1670)$.

Although results on kinematic fits to exclusive charged-current channels will be presented in another paper, we mention here that we find only one unambiguous fit[10] to the exclusive channel $\nu p \to \mu^-\Lambda 3\pi^+\pi^-$ (E_ν = 27 GeV). However, one of the $\pi^+\pi^-$ combinations has an invariant mass of 497 ± 4 MeV, and the event is therefore most likely an example of $\Delta S = 0$ associated production, $\nu p \to \mu^-\Lambda 2\pi^+\bar{K}^0$ with a close in $K^0_s \to \pi^+\pi^-$ decay. None of the three $\Lambda 2\pi^+\pi^-$ invariant masses (2019 ± 11, 2124 ± 11, 1780 ± 8) MeV or the $\Lambda 3\pi^+\pi^-$ mass (2286 ± 12 MeV) is near those of the previously observed $\Delta S = -\Delta Q$ BNL event.[11] Assuming zero observed events we calculate a 90% confidence level (c.l.) upper limit for $\Delta S = -\Delta Q$ $\nu p \to \mu^-\Lambda 3\pi^+\pi^-$ of 0.11% of the total charged-current neutrino rate with $E_\nu > 10$ GeV. Table III gives this rate as a function of neutrino energy.

We now compare our upper limit for this channel with the rate implied by the one observed BNL event. Since the neutrino

energy spectra for the two experiments are quite different, this comparison can be made only by assuming a particular energy dependence for the $\Delta S = -\Delta Q$ cross section. If we assume a threshold at 4 GeV and a constant cross section above threshold, the known fluxes and the BNL rate of 1 in 74[12] imply 10 events in our experiment. This is in poor agreement with our 2.3 events at the 90% confidence limit. If on the other hand the threshold is raised to 10 GeV, we expect 200 events in our experiment in strong disagreement with the BNL result.

IV. INCLUSIVE SINGLE-PARTICLE DISTRIBUTIONS

In figures 7(a) - 7(d) are presented the inclusive x, y, Q^2 and W distributions for the sample of charged-current events containing a V^o. Here - Q^2 is the square of the four-momentum transfer between the incident neutrino and outgoing muon, W is the total hadron effective mass, $x = Q^2/2m_p(E_\nu - E_\mu)$, and $y = (E_\nu - E_\mu)/E_\nu$. Also shown for comparison are the same distributions (solid curves) obtained from the total charged-current sample, where we have used events with 5 or more prongs to approximate the W distribution of the V^o sample. Figure 7(c) shows that the 5-prong selection results in similar W-distributions in all but the high W region. The dip at low y is a kinematic effect due to the fact that both the V^o sample and 5-prong sample tend to have higher values of W than the total charged-current sample. Within the present level of statistics there are no strong differences evident between the x, y and Q^2 distributions obtained

from the V^o sample and those obtained from the total charged-current sample.

To study the inclusive Λ and K^o production in more detail we have also employed variables normally used in analyzing hadron induced reactions. For the inclusive study of particle C produced in the hadronic reaction A + B → C + X one common set of variables is X_F and $P_\perp^2$, where X_F is the Feynman scaling variable $X_F = P_{||}^*/(\sqrt{s}/2)$. Here $P_\perp^2$ is the transverse 3-momentum squared of particle C with respect to the incident beam direction, $P_{||}^*$ is the component of particle C's momentum along the beam direction in the total center of mass system, (CMS) and $\sqrt{s}$ is the center of mass energy. In neutrino induced reactions the corresponding CMS frame is the hadronic rest system with beam direction defined as being opposite to the target proton direction in this system. The variables X_F and $P_\perp^2$ depend directly on the measured Λ and K^o momenta and can therefore be expected to be sensitive to differences between the Λ and K^o production mechanisms. Figures 8(b) and 8(d) show the inclusive $P_\perp^2$ distributions for the Λ and K_s^o samples separately. These distributions give good fits to simple $ae^{-bP_\perp^2}$ forms in the region $P_\perp^2 < 0.5$ $(GeV/c)^2$, yielding slope parameters $b = 7.1 \pm 1.4$ and $b = 5.8 \pm 1.1$ $(GeV/c)^{-2}$ respectively. These slopes are consistent with those found for inclusive hadron production from charged-current νp, $\bar{\nu} p$ interactions and μp interactions.[13,5,14]

The invariant X_F distributions $f(X_F) = (E^*/2W)dN/dX_F$ for the Λ and K_s^o samples are shown in figures 8(a) and 8(c). Here E^* is the V^o energy in the hadron rest system. The $f(X_F)$ distribution for the Λ sample clearly shows the tendency of the Λ to follow the proton direction while the K_s^o distribution is shifted towards the "beam-like" direction. The open triangles in Fig. 8(c) are taken from 6 GeV/c $\pi^+ p \to K_s^o X$ data[15] and are normalized to the ν data in the $-0.6 < X_F < 0.6$ region. Within the rather large errors the two distributions show the same qualitative behavior. The distributions of $< P_\perp >$ as a function of Q^2 and W are shown for the combined V^o sample in figures 9(a) and (b) respectively. A previous analysis using a subsample of the total charged-current data found that $< P_\perp >$ is approximately independent of Q^2 or W;[13] the distributions of figures 9(a) and (b) are consistent with this behavior.

Although the statistics are limited, we have attempted to gain an estimate of the Λ polarization effects in our inclusive charged-current sample. In the Λ rest frame we calculate the angles between the decay proton from the Λ and the incident neutrino direction θ_ν, the Λ direction θ_Λ, and the normal to the $\nu\Lambda$ production plane $\theta_\perp$. These last two angles have the advantage of being dependent on directly measured laboratory momenta only. Figure 10 shows the distributions of $\cos\theta_\nu$, $\cos\theta_\Lambda$ and $\cos\theta_\perp$ from which we calculate Λ-polarizations of (0.55 ± 0.40), (0.34 ± 0.33) and (0.23 ± 0.32) respectively.

V. INCLUSIVE INVARIANT MASS DISTRIBUTIONS - CHARM SEARCH

There is at present substantial evidence to support the existence of charmed particles. Observations of the non-leptonic decays of charmed particles have been made in e^+e^- colliding beam experiments[16,17,18,19] and possibly in a photoproduction experiment,[20] while signals from semi-leptonic decays may be present in ν and $\bar{\nu}$ induced dilepton events.[21] Using the quark-parton distributions of Field and Feynman[22] we estimate a rate of ~10% for charmed-particle production in νp interactions. Since in charmed particle decays the charmed-to-strange quark transition is favored, we might expect to see enhanced charmed-particle signals in events with final-state strange particles. On the other hand, a large number of competing charmed particle decay modes could dilute the signal in any one decay mode. We have searched for evidence of charmed particle production in our inclusive V^o data by looking in invariant mass distributions for signals from the non-leptonic decay of these particles into final-states containing Λ's and/or K^o's.

In Fig. 11(a) we show the $\Lambda 2\pi^+\pi^-$ invariant mass distribution for events with fewer than 9 prongs.[23] The data are presented in bins of 20 MeV width, which is the approximate limit of our resolution in the 2-2.5 GeV region. This distribution is of particular interest because of the observation from a photoproduction experiment of a signal at ~2.25 GeV in the $\bar{\Lambda}2\pi^-\pi^+$ state. In addition the $\Delta S = -\Delta Q$ event[11] had a $\Lambda 2\pi^+\pi^-$

mass combination at approximately this same value. There is no significant signal evident in Fig. 11(a) at ~2.25 GeV or in any other region. Attempts to observe a signal by plotting only combinations which contain a $\Sigma(1385)$ or by taking events in a restricted kinematic region (e.g. small x) were not succcessful. To obtain an estimate for producing a charmed particle at ~2.25 GeV, $C^+(2.25)$, we count all the events in the 2.2-2.3 GeV region (using all topologies) and obtain the following estimate for the upper limit on charmed particle production decaying into the $\Lambda 2\pi^+\pi^-$ final state:

$$\frac{\nu p \to \mu^- [C^+(2.25) \to \Lambda 2\pi^+\pi^-] X^+}{\nu p \to \mu^- X^{++}} < 1.0\% \text{ (90\% c.l. upper limit)}$$

where we have corrected for the neutral decay mode of the Λ.

In addition by taking as our signal only 5-pronged events which have a $\Lambda 2\pi^+\pi^-$ combination between 2.2 and 2.3 GeV, we can set the following limit for charmed particle production in the 2.2 to 2.3 GeV region for events having the same topology as the BNL event:

$$\frac{\nu p \to \mu^- [C^+(2.25) \to \Lambda 2\pi^+\pi^-] \pi^+ + \text{missing neutrals}}{\nu p \to \mu^- X^{++}} < 0.4\% \text{ (90\% c.l. upper limit)}$$

The invariant mass distribution for $\Lambda 3\pi^+2\pi^-$ is shown in Fig. 11(b). This distribution also fails to show any significant signals. For completeness Fig. 11(c) is the sum of the $\Lambda\pi^+$, $\Lambda 2\pi^+\pi^-$, and $\Lambda 3\pi^+2\pi^-$ mass distributions. This distribution would contain the signal for any +1 charged charmed baryon decaying through a $\Lambda m\pi$ final state. Except for the previously noted $\Sigma(1385)$ and the enhancements at 1.55 GeV and 1.85 GeV there are no other signals evident in this distribution.

We have searched without success for doubly-charged charmed baryons in the $\Lambda 2\pi^+$ and $\Lambda 3\pi^+\pi^-$ invariant mass distributions (figures 12(a) and 12(b) respectively) and for neutral charmed baryons in the $\Lambda\pi^+\pi^-$ and $\Lambda 2\pi^+2\pi^-$ invariant mass distributions (figures 12(c) and 12(d) respectively). If we interpret the BNL event as being an example of charm production $\nu p \rightarrow \mu^- C^{++}$, then the mass of the C^{++} is approximately 2.5 GeV. There are no signals at this value in figures 12(a) or 12(b). We note also that Knapp et al., (Ref. 20) reported an enhancement in the $\bar{\Lambda}$ $2\pi^+2\pi^-$ state at 2.5 GeV. The distribution of the invariant mass for the corresponding $\Lambda 2\pi^+2\pi^-$ state (Fig. 12(d)) shows no evidence for such an enhancement.

We have used our K_s^o data sample to search for evidence of D^o and D^+ production. We have searched for the D^o(or $\bar{D}^o$) in $K_s^o + (m\pi)^o$ invariant mass distributions (figures 13(a) and 13(b)) and for the D^+ (or $\overline{D^+}$) in $K_s^o + (m\pi)^\pm$ invariant mass distributions (figures 13(c)-13(e). The spike at ~1.25 GeV in Fig. 13(a) is due to multiple combinations from a few high multiplicity events.

There are no significant signals evident in the 1.8-1.9 GeV region in any of these distributions. In Fig. 14 we have added all the $K_s^o + (m\pi)^{\pm}$ distributions in the 1.5-2.5 GeV region. The solid curve in Fig. 14 is our estimate of the background in the 1.8-1.9 GeV region. Counting events above this background, correcting for the undetected K^o decay, and normalizing to the total charged-current sample, we obtain the following rate for D(1876) production:

$$\frac{\nu p \to \mu^- [D^{\pm} \to K^o (m\pi)^{\pm}] X}{\nu p \to \mu^- X^{++}} < 1.0\% \text{ (90\% c.l. upper limit).}$$

By using the previously measured $D^o \to \bar{K}^o \pi^+ \pi^-$ branching ratio[24] of ~4% and our zero observed events for this decay mode we obtain an upper limit of ~10% for total D^o production in νp charged-current interactions.

Finally, we have searched for F^+ production in our 2 K_s^o sample. The nonleptonic decays of this positive strangeness charmed meson should lead to strangeness equal zero $KK + m\pi$ states. The $(KK + m\pi)^+$ invariant mass distribution of Fig. 15 does not exhibit any significant signal for F production.

VI. SUMMARY

We have studied the properties of charged-current νp events having visible Λ's and K_s^o's in the final state. The rate for

producing events with at least one neutral strange particle is (14 ± 2)% of the total charged-current production. We observe signals from $\Sigma(1385)$ and possibly from $\Sigma(1670)$ and $\Sigma(1920)$. The inclusive x, y, Q^2 and W distribuitons for this restricted charged-current sample are found to be essentially the same as those distributions obtained from the total charged-current sample. We find no acceptable candidates for the $\Delta S = -\Delta Q$ production reaction $\nu p \to \mu^- \Lambda 3\pi^+\pi^-$.

We have searched for charmed-particle production by looking for signals in invariant mass distributions of particle combinations containing a Λ or K^o_s. We see no narrow ($\leq$ 50 MeV) signal greater than 10 events above background in any mass region. This leads to the following upper limits for charmed-particle production in any one mass region:

$$\frac{\nu p \to \mu^- [C \to K^o + m\pi] X}{\nu p \to \mu^- X^{++}} < 2\%$$

$$\frac{\nu p \to \mu^- [C \to \Lambda + m\pi] X}{\nu p \quad \mu^- X^{++}} < 1\%$$

where C is a particular charmed particle, and we have corrected for the neutral Λ and K^o decay modes. These rates can be reduced for particular mass regions.

REFERENCES

[1]J. Bell et al., "Experimental Study of Hadrons Produced in High Energy Neutrino-Proton Interactions" (to be submitted to Physical Rev. D). In selecting the muon we have used the F_2 and ϕ cuts, defined in Appendix B of the above reference. The bulk of the events were obtained using maximum beam intensity to increase the event rate in hydrogen. As a result the accidental background in the External Muon Identifier from neutrino interactions in the absorber became excessive. Under these conditions the kinematic selection method for muons is as efficient as the EMI and is applicable for a wider geometric coverage.

[2]"Scaling-Variable Distributions in Deep-Inelastic $\bar{\nu}$-p Interactions", S. J. Barish et al., Carnegie-Mellon University Preprint No. C00-3066-95 (submitted to Phys. Rev. D).

[3]There was one unique fit to $\bar{\Lambda} \to \bar{p}\pi^+$ and 4 fits ambiguous between K_s^o and $\bar{\Lambda}$. The χ^2 for these ambiguous fits all strongly favored the K_s^o interpretation, and therefore were taken as K_s^o fits.

[4]Further details of the two $3V^o$ events: (a) $[\Lambda\Lambda\bar{K}]$ 9 charged tracks at primary vertex, $\Sigma P_x > 69$ GeV, $E_\mu > 50$ GeV; (b) $[\Lambda K\bar{K}]$ 3 charged tracks at primary vertex, $\Sigma P_x = 29$ GeV, $E_\mu = 14$ GeV.

[5]"Properties of the Hadronic System Resulting from $\bar{\nu}$p Interactions", M. Derrick et al., (to be published in January 1, 1977 Phys. Rev. D).

[6]Y. G. Rjabov, Proceedings of the XVII International Conference on High Energy Physics, p. B120, Tbilisi, July 15-21, 1976.

[7]Note that for P_{inc} = 8.5 GeV/c, the cross section for $\pi^+p \to \Lambda K^+X + \Sigma^oK^+X$ equals .42 ± .09 mb while the cross section for $\pi^+p \to \Lambda K^oX + \Sigma^oK^oX$ = .17 ± .035 mb [Krebs (1970), Thesis, as referenced in LBL-53, May 1973]. However, data at 8 GeV/c [Aderholz et al., Nucl. Phys. B11, 259 (1969)] would imply that ΛK^+X is no more than ~1.7 times greater than ΛK^oX.

[8]The decay $\Sigma^+(1920) \to \Sigma^o\pi^+$, $\Sigma^o \to \Lambda\gamma$ [$\Sigma^+(1670) \to \Sigma^o\pi^+$, $\Sigma^o \to \Lambda\gamma$] will result in a $\Lambda\pi^+$ mass centered at ~1.85 [~1.55] GeV with a width of ~150 [~100] MeV. In general, any narrow mass state of mass M decaying via Σ^oX, $\Sigma^o \to \Lambda\gamma$, will yield a ΛX invariant mass which is less than M and broadened.

[9]Rutherford Lab - Imperial College Collaboration, Nucl. Phys. B119, 362 (1977).

[10]One other event fits $\nu p \to \Lambda$ + 5 prongs, but the event is ambiguous between the $\mu^-\Lambda K^+2\pi^+\pi^-$ and $\mu^-\Lambda 3\pi^+\pi^-$ final states.

[11]Cazzoli et al., Phys. Rev. Lett. 34, 1125 (1975).

[12]N. P. Samios, Proceedings of the 1975 International Symposium on Lepton and Photon Interactions (Stanford University) p. 527.

[13]Chapman et al., Phys. Rev. D14, 5 (1976).

[14]L. W. Mo, Proceedings of the 1975 International Symposium on Lepton and Photon Interactions (Stanford University) p. 651.

[15]D. J. Crennell et al., Phys. Rev. Lett. 28, 643 (1972).

[16]G. Goldhaber et al., Phys. Rev. Lett. 37, 255 (1976).

[17]I. Peruzzi et al., Phys. Rev. Lett. 37, 569 (1976).

[18]G. F. Feldman et al., Phys. Rev. Lett. 38, 1313 (1977).

[19]R. W. Brandelik et al., Phys. Lett. 70B, 132 (1977).

[20]Knapp et al., Phys. Rev. Lett. 37, 882 (1976).

[21]See, for example, references quoted in "Neutrino Physics at Fermilab", by F. A. Nezrick (Triangle Seminar). Fermilab-Conf-77/112-EXP, 7000.180 (to be published in Nuovo Cimento).

[22]R. D. Field and R. P. Feynman, Phys. Rev. D15, 2590 (1977).

[23]For high multiplicity events the number of $V^0(m\pi)$ combinations becomes excessive. In a 9-prong event, for example, there can be 30 $(V^0 2\pi^+\pi^-)$ combinations per V^0.

[24]I. Peruzzi et al., Phys. Rev. Lett. 39, 1301 (1977).

TABLE I

Number of uncorrected observed events for 1, 2, and V^0 final states.

$\nu p \rightarrow$ (a)	Observed Events
$\mu^- \left[\Lambda \rightarrow p\pi^-\right] X^{++}$	53
$\mu^- \left[K_s^0 \rightarrow \pi^+\pi^-\right] X^{++}$	64
$\mu^- \left[\Lambda \rightarrow p\pi^-,\ K_s^0 \rightarrow \pi^+\pi^-\right] X^{++}$	2
$\mu^- \left[K_s^0 \rightarrow \pi^+\pi^-,\ K_s^0 \rightarrow \pi^+\pi^-\right] X^{++}$	10
$\mu^- \left[\Lambda \rightarrow p\pi^-,\ K_s^0 \rightarrow \pi^+\pi^-,\ K_s^0 \rightarrow \pi^+\pi^-\right] X^{++}$	1
$\mu^- \left[\bar{\Lambda} \rightarrow \bar{p}\pi^+\right] X^{++}$	1
$\mu^- \left[\Lambda \rightarrow p\pi^-,\ \Lambda \rightarrow p\pi^-,\ K_s^0 \rightarrow \pi^+\pi^-\right] X^{++}$	1

(a) X^{++} does not contain a visible V^0 decay

TABLE II

Corrected number of events for particular final states.

$\nu p \rightarrow$ (a), (b)	Corrected No. of Events
$\mu^- \Lambda X^{++}$	82 ± 18
$\mu^- \Lambda K^o X^{++}$	0 ± 27
$\mu^- K^o X^{++}$	66 ± 49
$\mu^- K^o K^o X^{++}$	85 ± 31

(a) X^{++} does not contain a neutral strange particle, but could contain charged strange particles (e.g., K^-).

(b) K^o may be either K^o or $\bar{K}^o$.

TABLE III

Upper limits for the reaction $\nu p \to \mu^- \Lambda 3\pi^+\pi^-$ as a function of neutrino energy.

Energy Range	$(\nu p \to \mu^- \Lambda 3\pi^+\pi^-)/\nu p \to cc^*$
E_ν > 10 GeV	0.11%
> 15 GeV	0.13%
> 20 GeV	0.15%
> 25 GeV	0.19%
> 30 GeV	0.23%

*90% confidence level upper limits based on zero observed events.

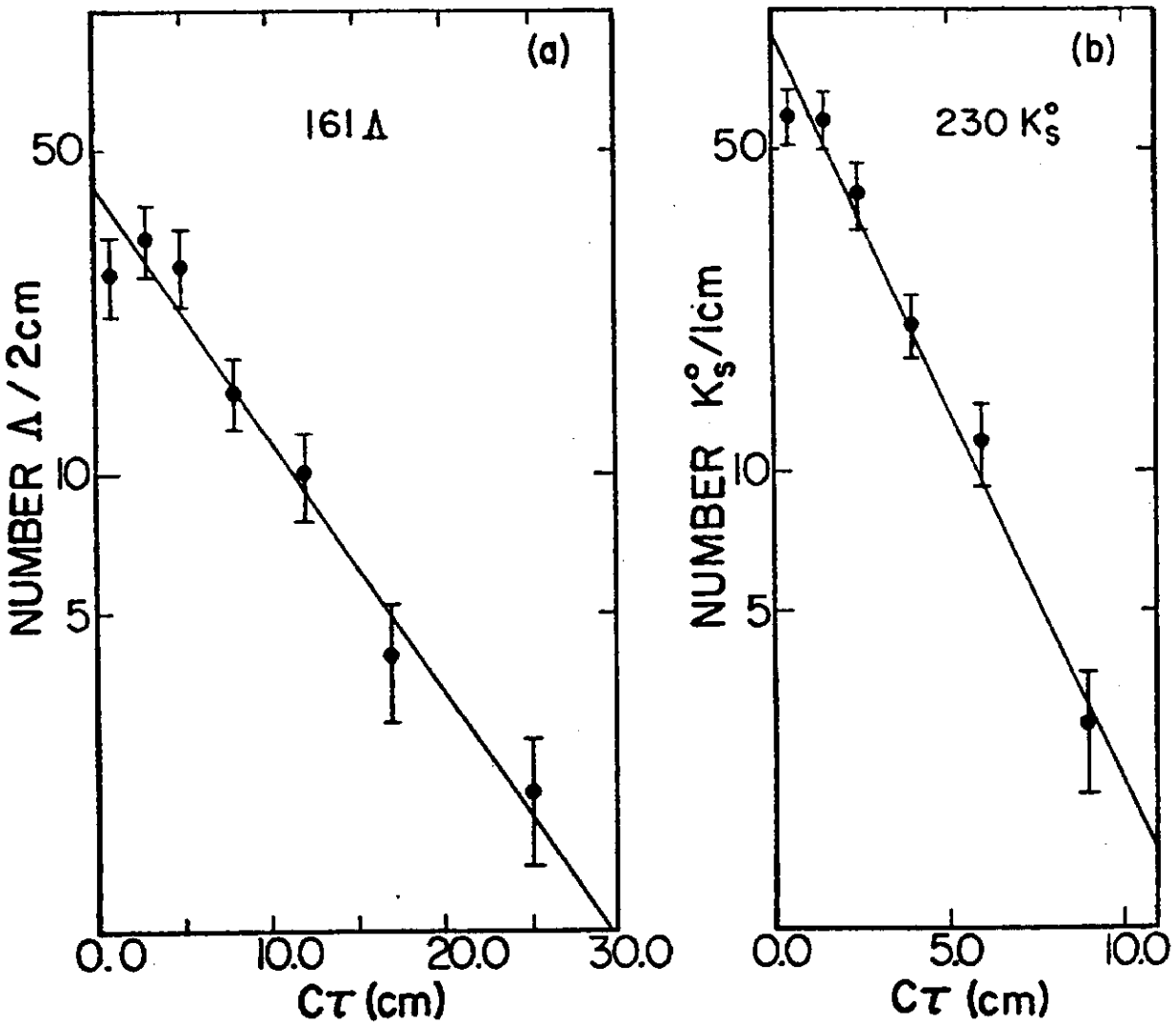

Fig. 1: Distribution of $c\tau$ (τ = proper decay time) for (a) Λ and (b) K^0_s decays.

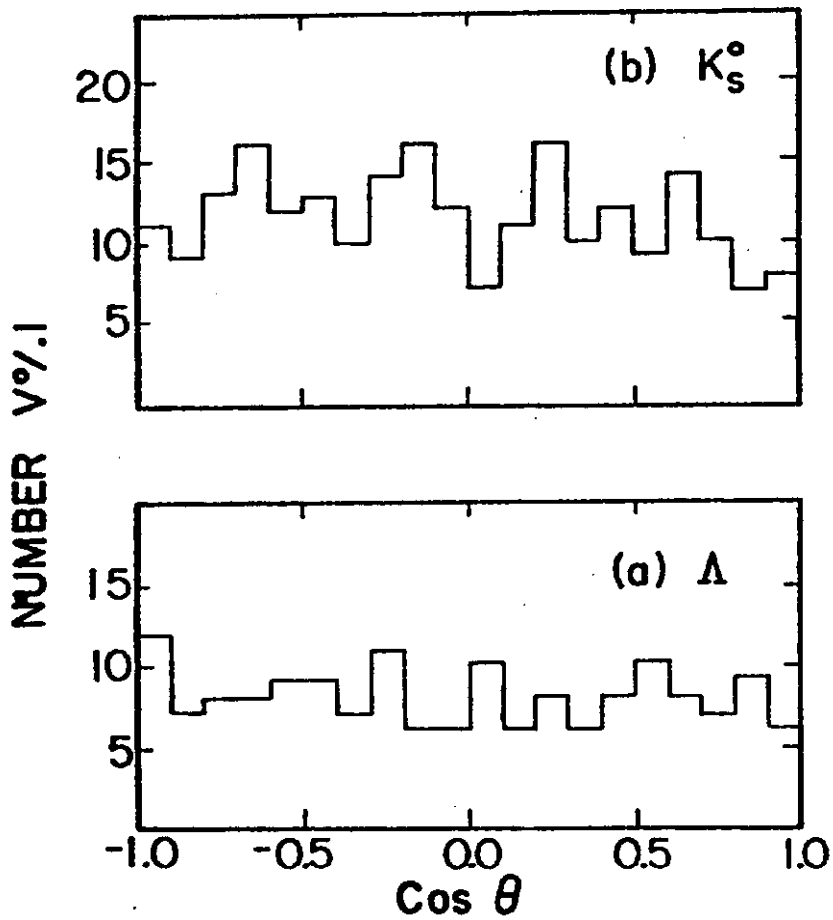

Fig. 2: Distribution of cosθ for (a) Λ and (b) K_s^o decays. Here θ is the decay angle of the $p(\pi^+)$ from the $\Lambda(K_s^o)$ decay with respect to the $\Lambda(K_s^o)$ direction in the lab, calculated in the $\Lambda(K_s^o)$ rest frame.

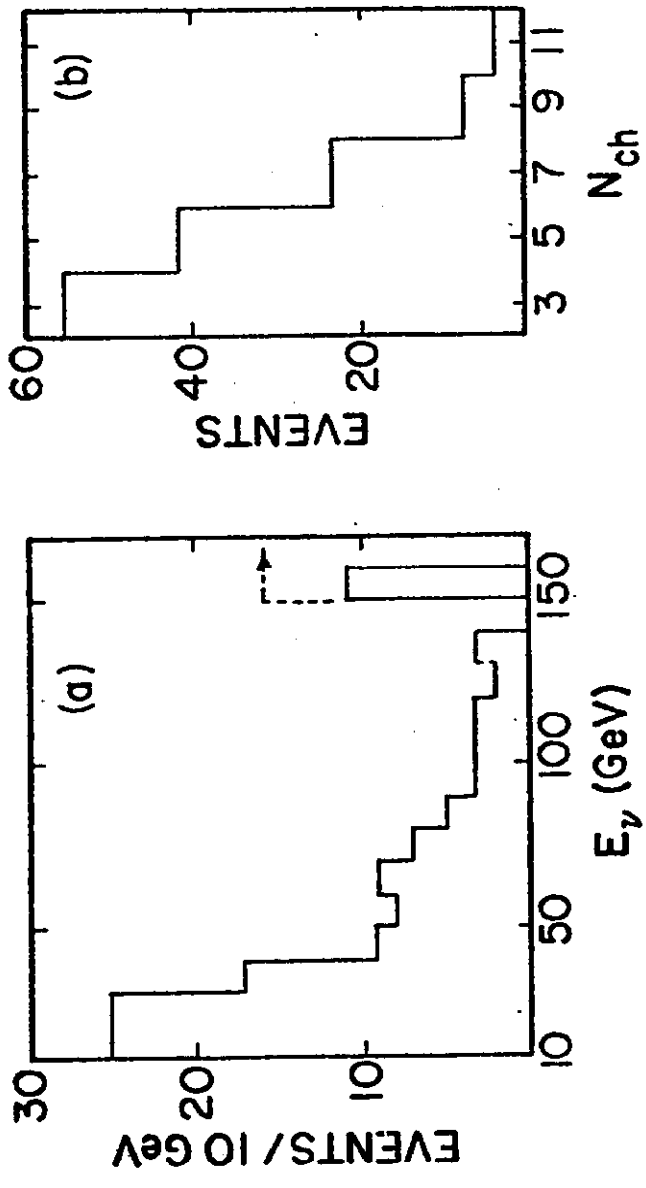

Fig. 3: (a) Distribution of neutrino energy E_ν for the 132 charged-current V^0 events. (b) Distribution of the charged multiplicity for the same events.

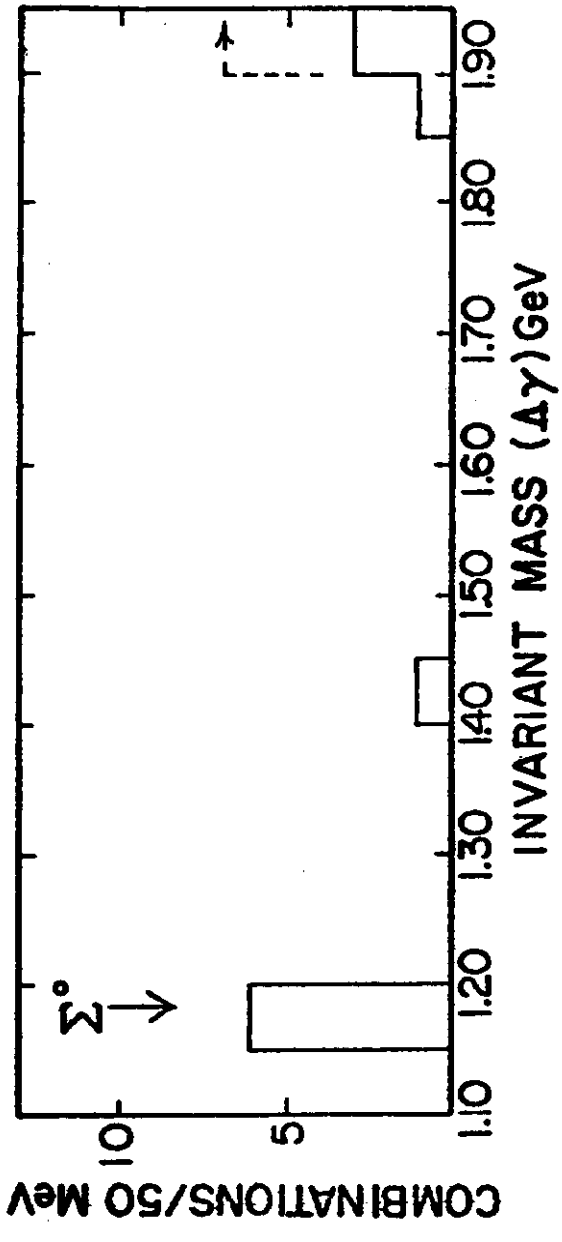

Fig. 4: Distribution of the Λγ invariant mass for the V^0 charged-current events.

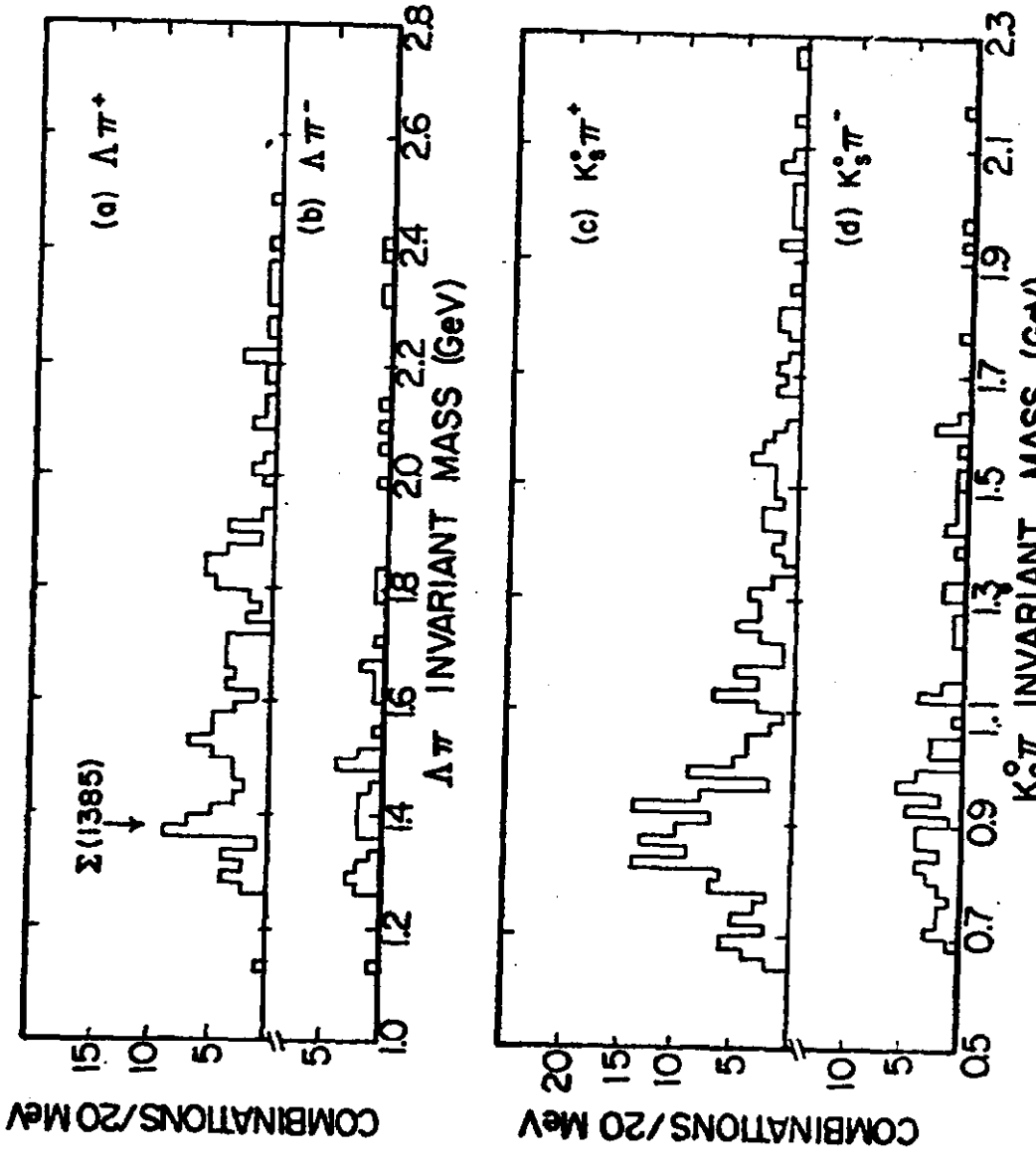

Fig. 5: Invariant mass distributions for (a) $\Lambda\pi^+$ (b) $\Lambda\pi^-$ (c) $K^0_s\pi^+$ (d) $K^0_s\pi^-$.

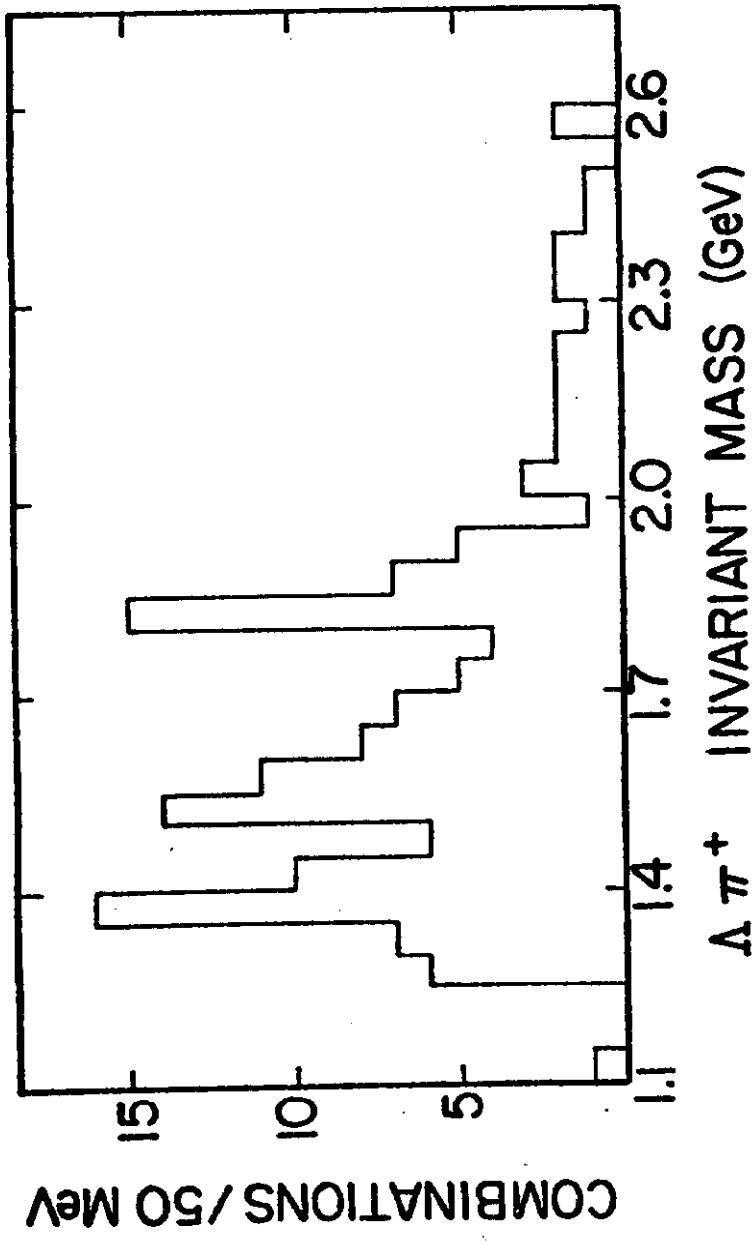

Fig. 6: The $\Lambda\pi^+$ invariant mass distribution (Fig. 5a), redrawn with 50 MeV bins.

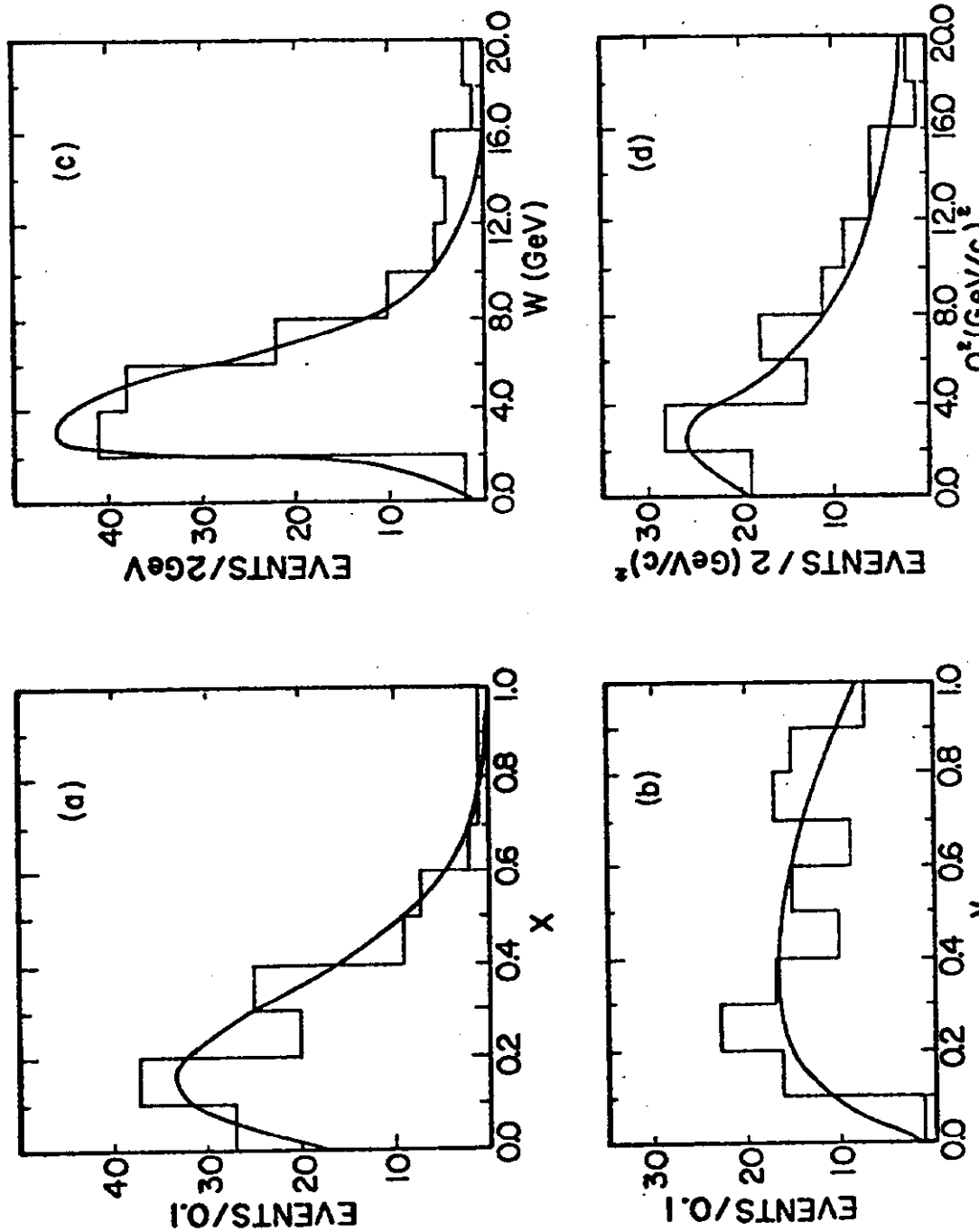

Fig. 7. (a) - (d). The x, y, W, and Q^2 distributions respectively for the charged-current V^0 events. The solid curves are the same distributions for the total charged-current sample having 5 or more prongs, normalized to the number of V^0 events.

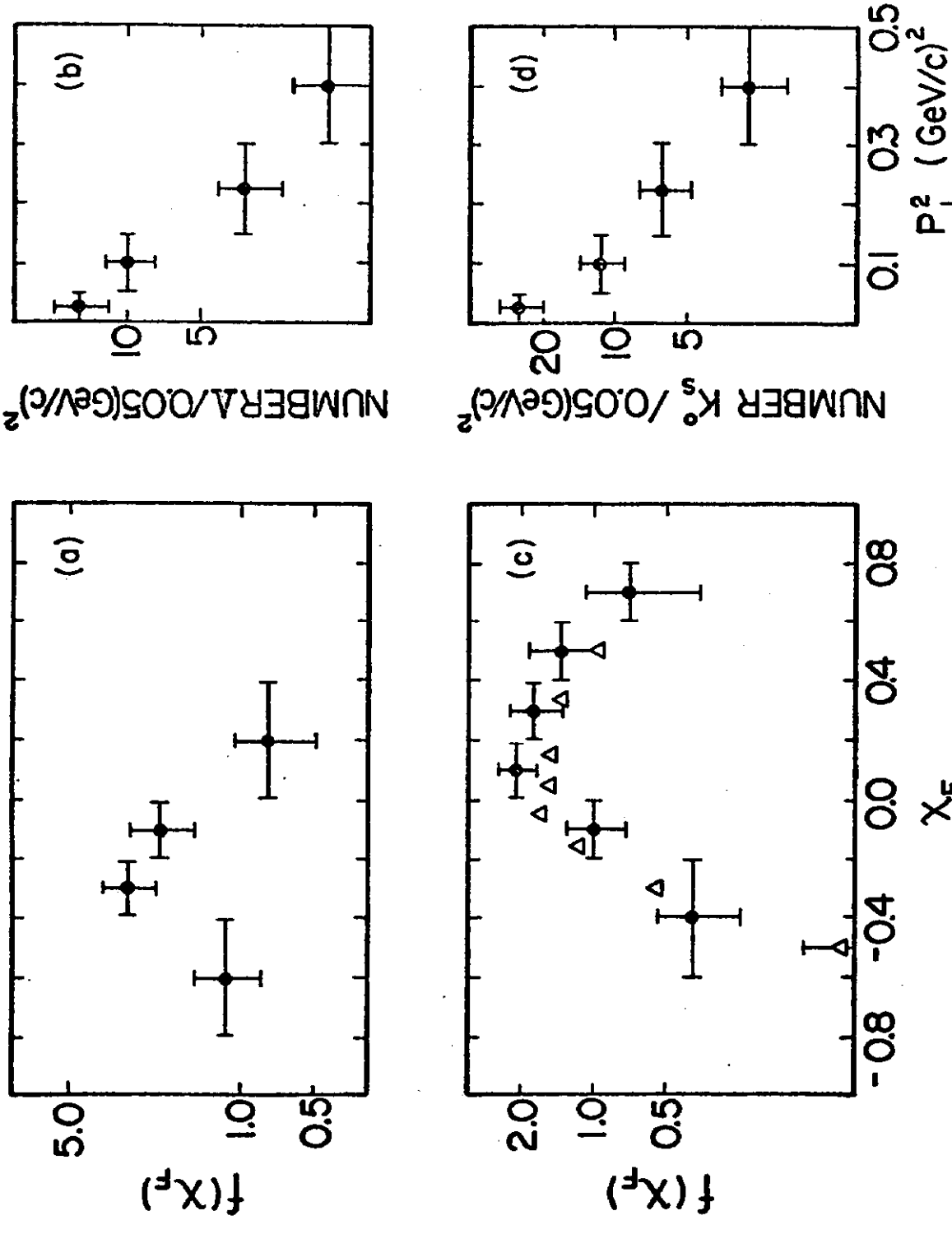

Fig. 8. (a) and (b): The $f(X_F)$ and $P_\perp^2$ distributions respectively for the inclusive Λ events. (c) and (d): The same distributions for the inclusive K_s^o sample. Here $f(X_F) \equiv (E^*/2W)\,dN/dX_F$, where E^* is the V^o energy in the hadron rest system. In (c) the open triangles are taken from $\pi^+ p \to K_s^o X$ data at 6 GeV/c, and are normalized in the region $-0.6 < X_F < 0.6$.

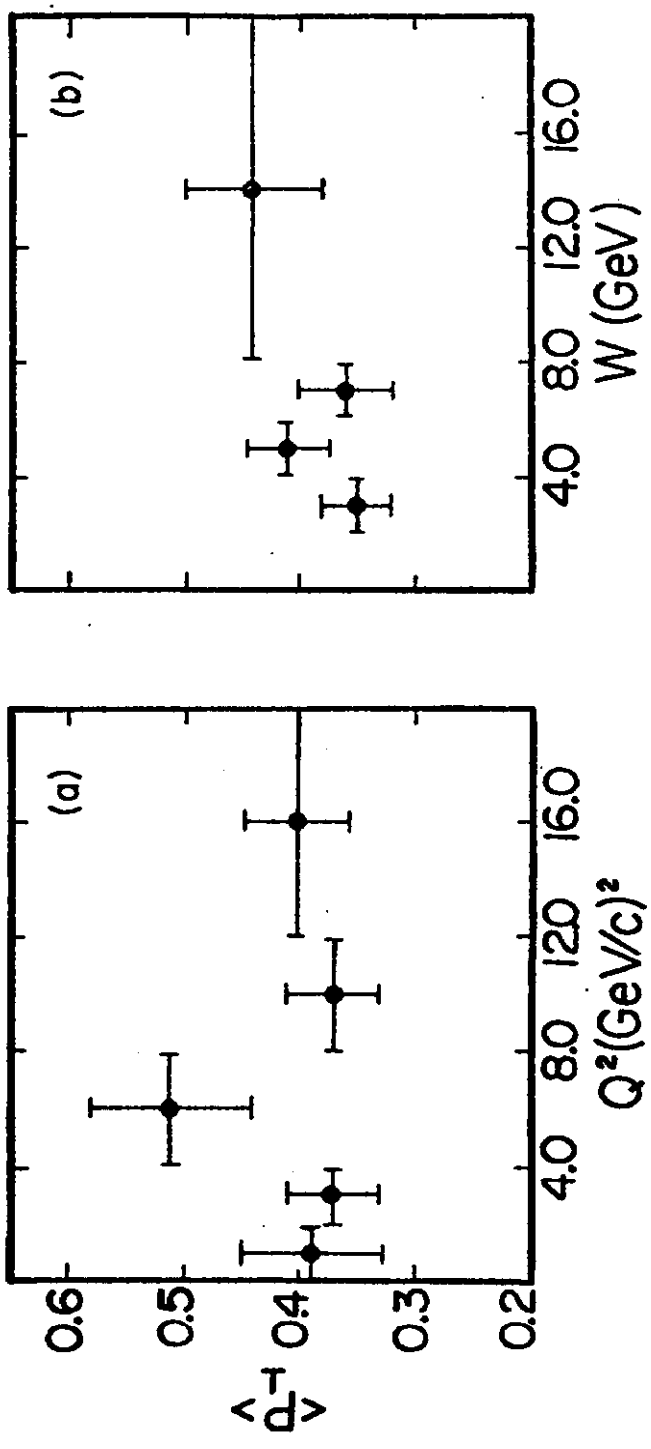

Fig. 9: Distributions of $\langle P_T \rangle$ as a function of (a) Q^2 and (b) W for the charged current V^0 sample.

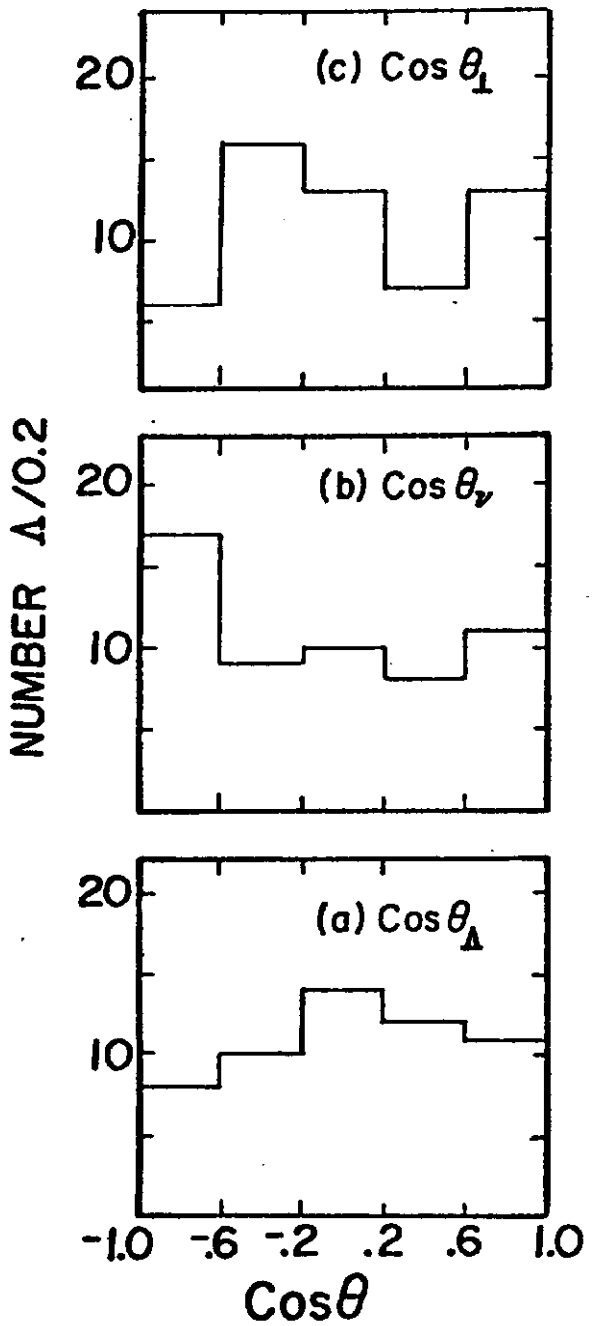

Fig. 10: Distribution of the cosine of the proton decay angle calculated in the Λ rest frame with respect to (a) the incident neutrino direction, (b) the Λ direction and (c) the normal to the νΛ production plane.

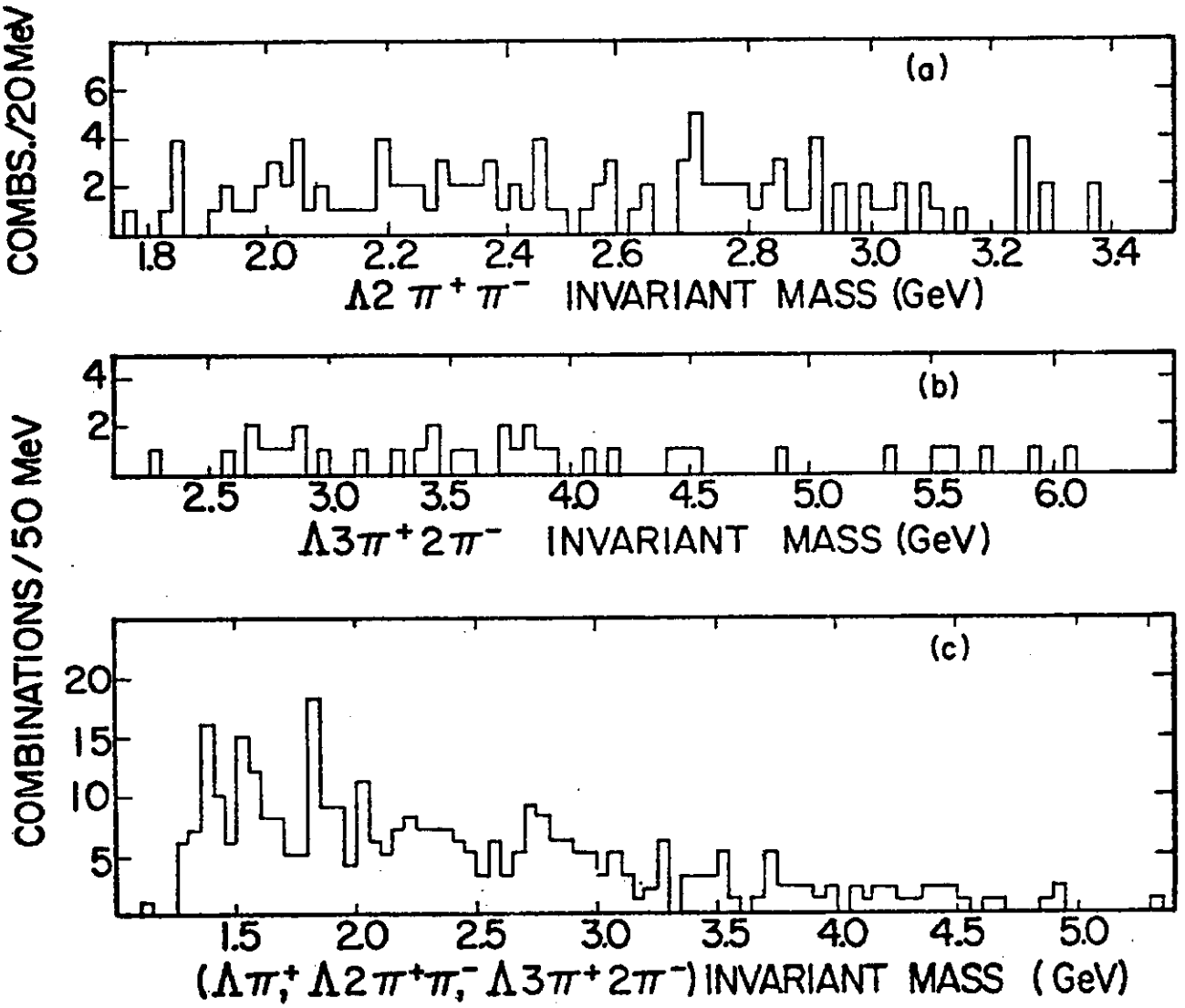

Fig. 11: (a) the $\Lambda 2\pi^+\pi^-$ invariant mass distribution
(b) the $\Lambda 3\pi^+ 2\pi^-$ invariant mass distribution
(c) the sum of the $\Lambda\pi^+$, $\Lambda 2\pi^+\pi^-$ and $\Lambda 3\pi^+ 2\pi^-$ invariant mass distributions.

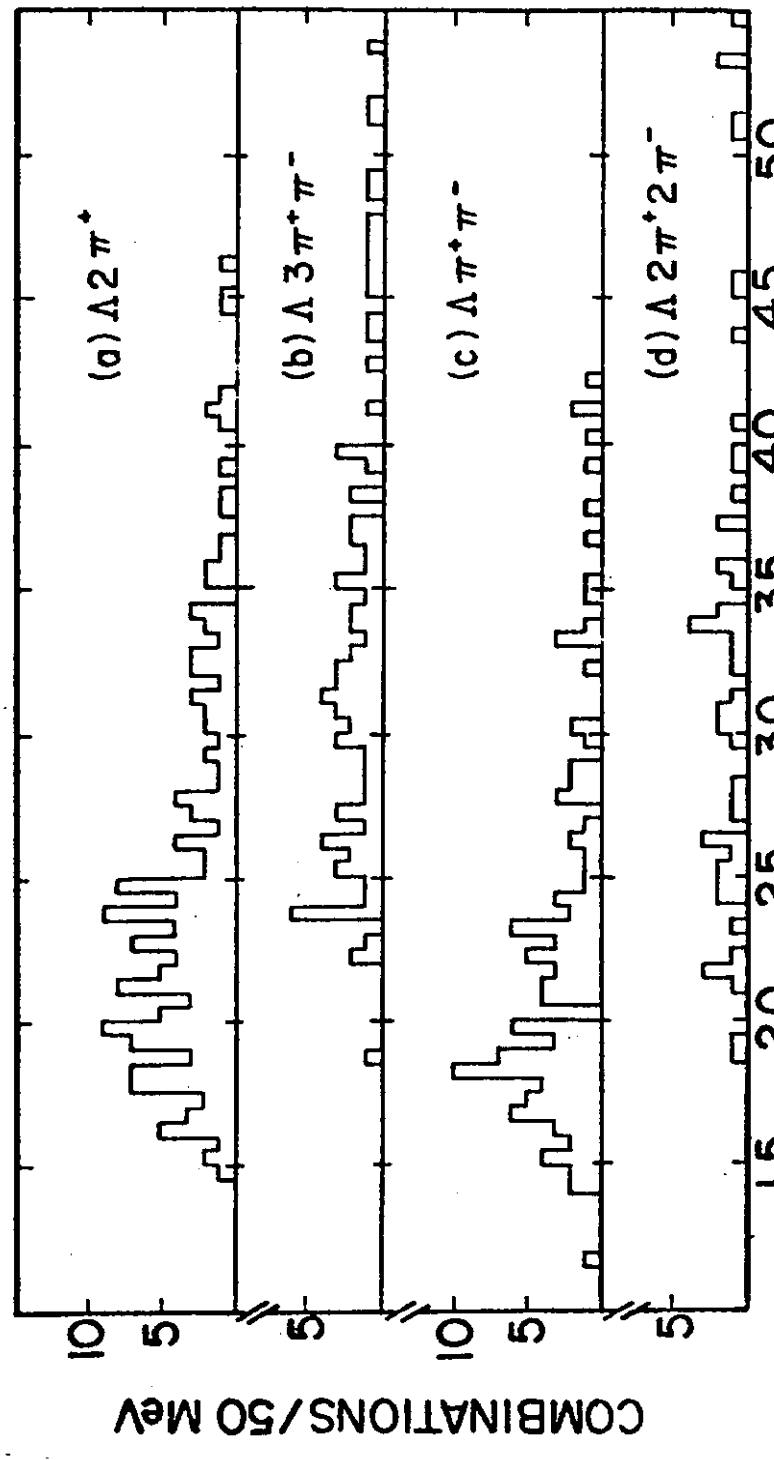

Fig. 12: The invariant mass distribution for (a) $\Lambda 2\pi^+$, (b) $\Lambda 3\pi^+\pi^-$, (c) $\Lambda\pi^+\pi^-$, (d) $\Lambda 2\pi^+ 2\pi^-$.

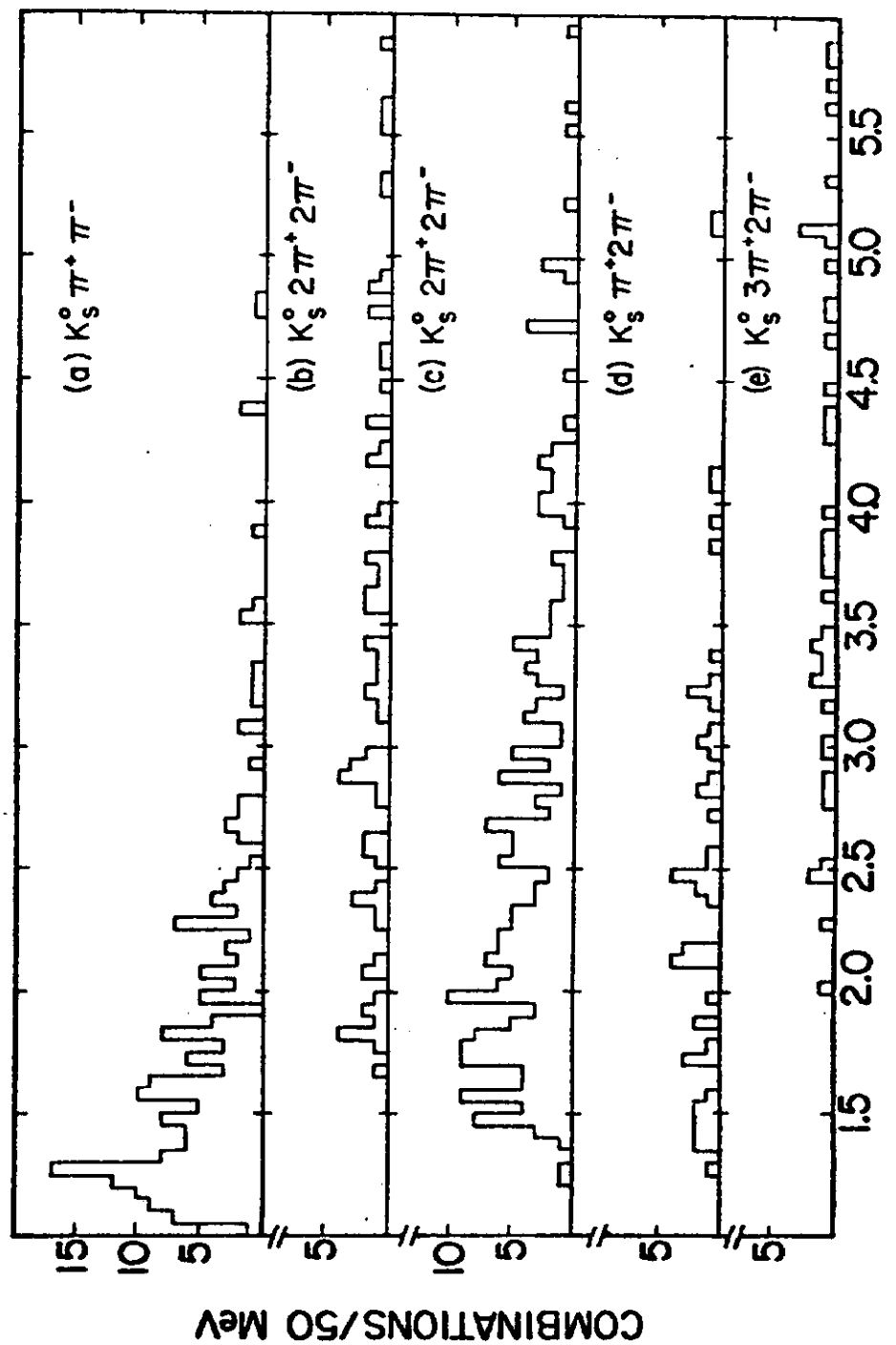

Fig. 13: The invariant mass distribution for (a) $K^o_s \pi^+ \pi^-$,
(b) $K^o_s 2\pi^+ 2\pi^-$, (c) $K^o_s 2\pi^+ \pi^-$, (d) $K^o_s 3\pi^+ \pi^-$, (e) $K^o_s \pi^+ 2\pi^-$

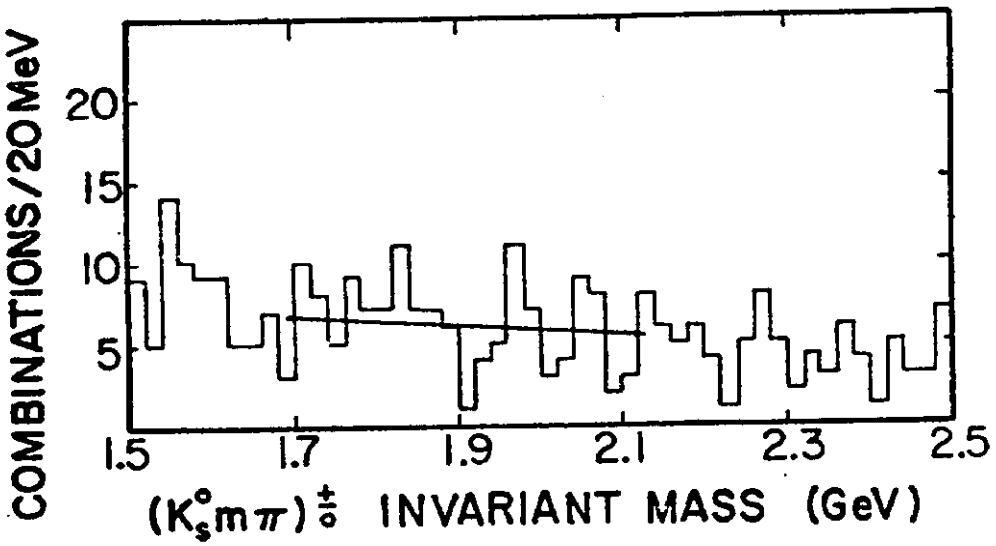

Fig. 14: The combined K^0_s $(m\pi)^{\pm}_0$ invariant mass distributions in the 1.5-2.5 GeV region.

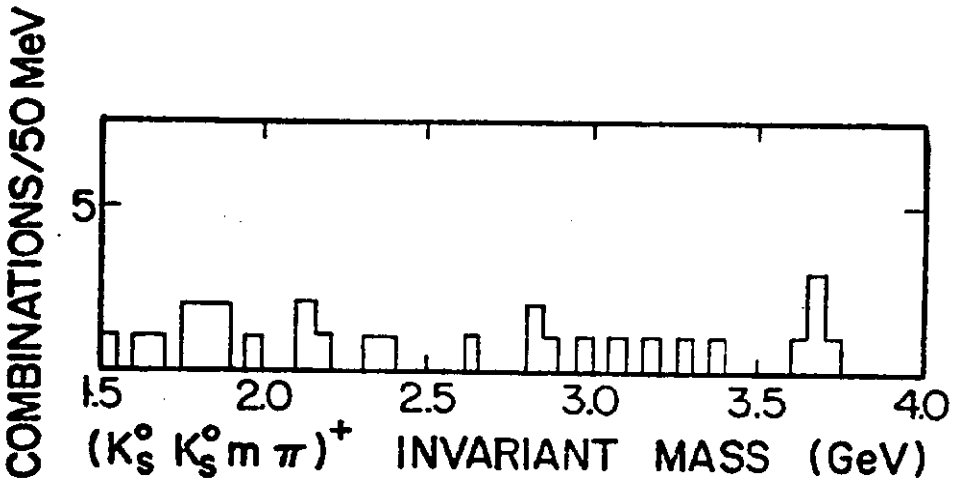

Fig. 15: The combined $(K^0_S K^0_S m\pi)^+$ invariant mass distributions.